


Evidence for Suppression of Structure Growth in the Concordance Cosmological Model

Nhat-Minh Nguyen^{Ⓧ,*}, Dragan Huterer^{Ⓧ,†} and Yuewei Wen^{Ⓧ,‡}

*Leinweber Center for Theoretical Physics, University of Michigan, 450 Church Street, Ann Arbor, Michigan 48109-1040, USA
and Department of Physics, College of Literature, Science and the Arts, University of Michigan,
450 Church Street, Ann Arbor, Michigan 48109-1040, USA*

 (Received 11 February 2023; revised 5 June 2023; accepted 7 August 2023; published 11 September 2023)

We present evidence for a suppressed growth rate of large-scale structure during the dark-energy-dominated era. Modeling the growth rate of perturbations with the “growth index” γ , we find that current cosmological data strongly prefer a higher growth index than the value $\gamma = 0.55$ predicted by general relativity in a flat Lambda cold dark matter cosmology. Both the cosmic microwave background data from Planck and the large-scale structure data from weak lensing, galaxy clustering, and cosmic velocities separately favor growth suppression. When combined, they yield $\gamma = 0.633^{+0.025}_{-0.024}$, excluding $\gamma = 0.55$ at a statistical significance of 3.7σ . The combination of $f\sigma_8$ and Planck measurements prefers an even higher growth index of $\gamma = 0.639^{+0.024}_{-0.025}$, corresponding to a 4.2σ tension with the concordance model. In Planck data, the suppressed growth rate offsets the preference for nonzero curvature and fits the data equally well as the latter model. A higher γ leads to a higher matter fluctuation amplitude S_8 inferred from galaxy clustering and weak lensing measurements, and a lower S_8 from Planck data, effectively resolving the S_8 tension.

DOI: 10.1103/PhysRevLett.131.111001

Introduction.—The flat Lambda cold dark matter (Λ CDM) concordance cosmology, which combines general relativity (GR) and a spatially flat universe with $\sim 70\%$ constant dark energy and $\sim 30\%$ cold dark matter, provides an excellent fit to observational data. However, several tensions in the measurements of parameters in this model have been noted in recent years [1]. Most significantly, the expansion rate H_0 inferred from the distance ladder [2] is higher than that measured by the cosmic microwave background (CMB) [3]. At a lesser significance, the parameter $S_8 \equiv \sigma_8 \sqrt{\Omega_m}/0.3$ (where σ_8 is the amplitude of mass fluctuations in spheres of $8 h^{-1}$ Mpc with $h = H_0/100 \text{ km s}^{-1} \text{ Mpc}^{-1}$, and Ω_m is matter density relative to the critical density) determined by CMB observations is larger than that found by galaxy clustering and weak gravitational lensing measurements [4]. Finally, the Planck CMB data themselves show a preference for a nonzero spatial curvature Ω_K [3].

In this Letter, we consider the possibility that the growth of structure deviates from the concordance model. While $(\Omega_m, S_8, \text{ and } \Omega_K)$ affect the growth of density perturbations, they also control geometrical quantities like distances and volumes, complicating the physical interpretation. It is thus important to isolate and constrain the growth of structure [5] separately from geometrical quantities. Here, we adopt a precise parametrization of the growth rate and find evidence for growth suppression—relative to the expectation from flat Λ CDM and GR—which also reconciles tensions in S_8 and Ω_K constraints. Our results clarify

and consolidate the current situation in the field, where different analyses adopting different prescriptions of growth (and geometry) either found some evidence for a suppressed growth [6–16] or did not [17–26]. Our baseline constraint is consistent with Refs. [19–23], whose constraints are also consistent with standard growth rate in Λ CDM and GR given their data and modeling uncertainties.

Growth of structure.—Over cosmic time, matter density fluctuations $\delta \equiv (\rho - \bar{\rho})/\bar{\rho}$ (where ρ and $\bar{\rho}$ are the local and the cosmic mean densities, respectively) are amplified by gravity. Assuming GR and restricting to the linear regime where $\delta \ll 1$ ($k \lesssim 0.1 h \text{ Mpc}^{-1}$ today) and subhorizon scales ($k \gtrsim H_0 \simeq 0.0003 h \text{ Mpc}^{-1}$ today), we can describe the growth of large-scale structure as [27,28]

$$\ddot{\delta}(\mathbf{k}, t) + 2H\dot{\delta}(\mathbf{k}, t) - 4\pi G\bar{\rho}\delta(\mathbf{k}, t) = 0, \quad (1)$$

where the dot denotes the derivative with respect to time; the matter overdensity δ , the expansion rate H , and the mean matter density $\bar{\rho}$ all depend on time, while every Fourier \mathbf{k} mode evolves independently. Linear growth is thereby described by the linear growth function $D(t) \equiv \delta(t)/\delta(t_0)$, where t_0 denotes the present, and the growth rate $f(a) \equiv d \ln D(a)/d \ln a$, where $a(t)$ is the scale factor. The growth rate is a central link between data and theory: It is proportional to large-scale structure observables like peculiar velocities and redshift-space distortions [29,30], while being exquisitely sensitive to the properties of dark-energy models [31].

To isolate the temporal evolution of structure, Refs. [32–34] introduced a robust and accurate approximation of the growth rate as

$$f(a) = \Omega_m^\gamma(a), \quad (2)$$

where γ is the growth index. In particular, Refs. [33,34] showed that standard GR in the flat Λ CDM background predicts $\gamma \simeq 0.55$ even in the presence of dark energy; this fit is accurate to $\simeq 0.1\%$ [34–36]. A measured deviation from $\gamma = 0.55$ would suggest an inconsistency between the concordance cosmological model and observations.

Assuming Eq. (2), the linear growth function takes the form

$$D(\gamma, a) = \exp \left[- \int_a^1 da \frac{\Omega_m^\gamma(a)}{a} \right], \quad (3)$$

where we have normalized $D(\gamma, a = 1) \equiv 1$ for all γ . A $\gamma > 0.55$ corresponds to a growth rate $f(\gamma, a) < f(0.55, a)$ and, for our present-day normalization, to a growth function $D(\gamma, a) > D(0.55, a)$ in the past.

Methodology and data.—To implement Eqs. (2) and (3), we express the linear matter power spectrum as

$$P(\gamma, k, a) = P_{\text{today}}(k, a = 1) D^2(\gamma, a), \quad (4)$$

where P_{today} is the fiducial linear matter power spectrum evaluated today which depends on the usual set of cosmological parameters. We note that the choice of $a(t)$ at which growth is normalized does not impact our γ constraints and its (in)consistency with $\gamma = 0.55$ as we jointly infer the power spectrum amplitude as well (see below). To compute the transfer functions and power spectra, we modify the cosmological Boltzmann solver CAMB [37,38]. With $\gamma = 0.55$, we obtain (at redshift $z = 1.5$ and up to $k \lesssim 0.1 \text{ h Mpc}^{-1}$) linear matter power spectra within 0.1% of the outputs from the unmodified version of CAMB. Likewise, we repeat the baseline Planck 2018 [3] and Dark Energy Survey (DES) year-one [39] analyses, using our modified CAMB [40] at fixed $\gamma = 0.55$ and reproduce their constraints on relevant cosmological parameters well within their precision.

Because the growth-index parametrization has only been validated for subhorizon perturbations, care needs to be taken when modeling the CMB whose information partially comes from large scales and high redshifts. Therefore, we isolate the effect of γ from the prediction for the (unlensed) primary CMB anisotropies. Equation (4) only modifies the CMB lensing gravitational potential [41], which is generated by density fluctuations within the regime where Eqs. (2)–(4) are valid.

Our baseline data include measurements of the parameter combination $f\sigma_8$ from peculiar velocity and redshift-space distortion data, at local ($z < 0.1$) [11,44–47] and

cosmological distances ($z \geq 0.1$) [48–53]. Figure 2 shows these $f\sigma_8$ measurements at the corresponding redshifts. We assume that the $f\sigma_8$ measurement uncertainties are Gaussian distributed and uncorrelated among each other [54]. We further complement the $f\sigma_8$ measurements with either the Planck 2018 CMB data—including CMB temperature-temperature (TT), temperature-polarization plus polarization-polarization spectra, and CMB lensing reconstruction [3,55,56] (hereafter, PL18 collectively)—or large-scale structure data from galaxy surveys, or both. Data from galaxy surveys include (a) the DESY1 3x2pt correlation functions [39] (hereafter DESY1) and (b) baryon acoustic oscillations in the 6dF Galaxy Survey (6dFGS) galaxy [57] and the Sloan Digital Sky Survey (SDSS) [53,58,59] galaxy plus Lyman-alpha (hereafter, BAO collectively). When including both SDSS $f\sigma_8$ and BAO data, we employ joint covariance and likelihood that properly account for their correlations [60]. Throughout, we adopt the same likelihoods and priors used in the baseline of those analyses. We fix the total mass of neutrinos to $\sum m_\nu = 0.06 \text{ eV}$ and include neutrino contribution Ω_ν in the matter density parameter Ω_m . We verify that excluding Ω_ν in computing theoretical $f\sigma_8$ leads to negligible changes in the latter and all downstream results. We allow γ to vary assuming a uniform prior $\mathcal{U}(0, 2.0)$.

We constrain the growth index γ along with other standard cosmological parameters: the matter and baryon densities relative to critical Ω_m and Ω_b , the Hubble constant H_0 , spectral index n_s , mass fluctuation amplitude σ_8 , and reionization optical depth τ . We therefore perform Bayesian inference via the Markov chain Monte Carlo (MCMC) method using the COBAYA framework [61] and analyze the MCMC samples using the GetDist package [62].

To quantify the statistical significance of our results, we compute the Bayesian factor of $\gamma = 0.55$ and $\gamma \neq 0.55$ by assuming the Savage-Dickey density ratio

$$\log_{10} \text{BF}_{01} = \log_{10} \frac{\mathcal{P}(\gamma|d, M_1)}{\mathcal{P}(\gamma|M_1)} \Big|_{\gamma=0.55}, \quad (5)$$

where d and M_1 , respectively, denote the data and the model with γ , while $\mathcal{P}(\gamma|M_1) = \mathcal{U}(0., 2.)$. This is reported in the fifth column of Table I. We further quote the significance of $\gamma \neq 0.55$ following the two-tailed test and measuring the posterior tail in units of Gaussian sigmas. In the Supplemental Material [63], we compare the goodness of fit of the models with respect to each data combination and for each individual likelihood.

Constraints on γ in a flat universe.—We first consider the data combination $f\sigma_8 + \text{PL18}$. Marginalizing over all other cosmological parameters, we obtain the orange posterior density in Fig. 1. This corresponds to the constraint $\gamma = 0.639_{-0.025}^{+0.024}$ and a Bayes factor of $|\log_{10} \text{BF}_{01}| = 1.7$. The former excludes $\gamma = 0.55$ at a statistical significance of 4.2σ , while the latter provides “very strong” evidence for

TABLE I. Constraints on the growth index γ and cosmological parameters S_8 and H_0 from different data combinations, the corresponding Bayes factors, and chi-square differences relative to the concordance model ($\gamma = 0.55$).

Data	γ	S_8	H_0 (kms $^{-1}$ Mpc $^{-1}$)	$ \log_{10}\text{BF}_{10} $	$\Delta\chi^2 \equiv \chi^2_{\gamma} - \chi^2_{\gamma=0.55}$
PL18	0.668 $^{+0.068}_{-0.067}$	0.807 $^{+0.019}_{-0.019}$	68.1 $^{+0.7}_{-0.7}$	0.4	-2.8
PL18 + $f\sigma_8$	0.639 $^{+0.024}_{-0.025}$	0.814 $^{+0.011}_{-0.011}$	67.9 $^{+0.5}_{-0.5}$	1.7	-13.6
PL18 + $f\sigma_8$ + DESY1 + BAO	0.633 $^{+0.025}_{-0.024}$	0.802 $^{+0.008}_{-0.008}$	68.4 $^{+0.4}_{-0.4}$	1.2	-13.2
PL18 + $f\sigma_8$ + DESY1 + BAO (flat Λ CDM + GR)	0.55	0.803 $^{+0.008}_{-0.008}$	68.5 $^{+0.4}_{-0.4}$		0

deviation from the GR + flat Λ CDM prediction of $\gamma = 0.55$ according to the Jeffreys scale [64]. Neither PL18 nor $f\sigma_8$ alone substantially constrains the growth index due to degeneracies with other cosmological parameters, yet together they show a clear preference for $\gamma > 0.55$, that is, a lower rate of growth than predicted by GR in flat Λ CDM. Figure 2 illustrates the effect of growth suppression as a function of the redshift by showing the $f(z)\sigma_8(z)$ posterior assuming flat Λ CDM and assuming flat Λ CDM + γ , both inferred from the $f\sigma_8$ + PL18 data combination.

Next, we investigate how the galaxy clustering and lensing data constrain γ . To do so, we replace the PL18 data by the DESY1 3x2pt measurements of galaxy clustering and weak lensing, together with the expansion-history data from BAO. The $f\sigma_8$ + DESY1 + BAO data combination yields the marginalized constraint $\gamma = 0.598^{+0.031}_{-0.031}$. Much like the $f\sigma_8$ + PL18 constraint, this combination prefers a higher growth index than the GR value, except now at a lower statistical significance, excluding $\gamma = 0.55$ at 2.0σ .

We finally report the constraint from all data combined, $f\sigma_8$ + PL18 + DESY1 + BAO:

$$\gamma = 0.633^{+0.025}_{-0.024}. \quad (6)$$

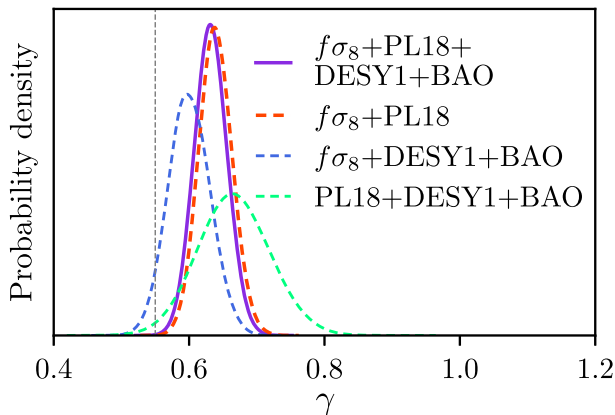


FIG. 1. Marginalized constraints on the growth index γ from CMB (PL18) and LSS data. The latter includes $f\sigma_8$, DESY1, and BAO measurements. The legend indicates different combinations of the datasets. The vertical dashed line marks the concordance model prediction of $\gamma = 0.55$.

An analysis of the posterior tails indicates that $\gamma = 0.55$ is excluded at 3.7σ , while the Bayes factor $|\log_{10}\text{BF}| = 1.2$ shows “strong” evidence for a departure from the expected value of γ . The constraint is represented by the violet posterior density in Fig. 1; it is very close to the posterior for $f\sigma_8$ + PL18. For clarity, we additionally plot the γ constraint from PL18 + DESY1 + BAO in green.

We summarize all γ constraints, together with their statistical significance, in Table I. We further assert the robustness of and internal consistency between our γ constraints in the Supplemental Material [63].

Implications for S_8 tension.—A moderate yet persistent tension in constraints of S_8 has emerged between CMB measurements, e.g., Planck [3] or Atacama Cosmology Telescope plus Wilkinson Microwave Anisotropy Probe [65], and low-redshift 3x2pt measurements of weak lensing and galaxy clustering, e.g., the DES [39], the Kilo-Degree Survey [66], and combinations thereof [67]. This discrepancy is statistically significant and unlikely to be explained by lensing systematics alone [68]; thus, it motivates investigations of physics beyond the standard model.

Figure 3 shows the marginalized constraints in the 2D planes of the growth index γ and, from left to right, S_8 or

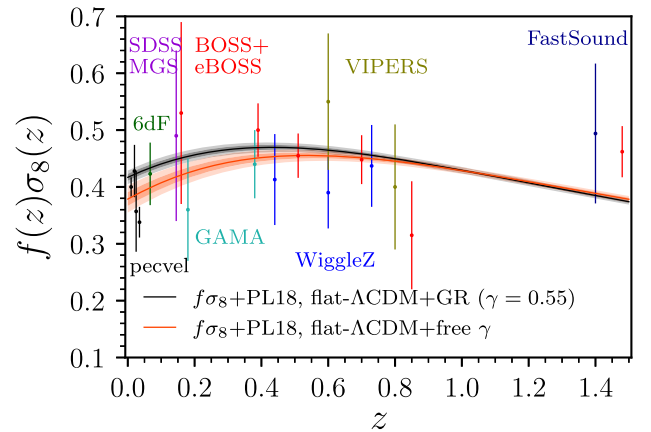


FIG. 2. Marginalized posterior on the theoretical $f(z)\sigma_8(z)$ assuming the growth-index parametrization in Eq. (2). Shaded bands show the 68% and 95% posteriors from our baseline analysis that includes $f\sigma_8$ and PL18 data (orange), and the corresponding constraints in the concordance model with $\gamma = 0.55$ (black). The data points indicate actual $f\sigma_8$ measurements.

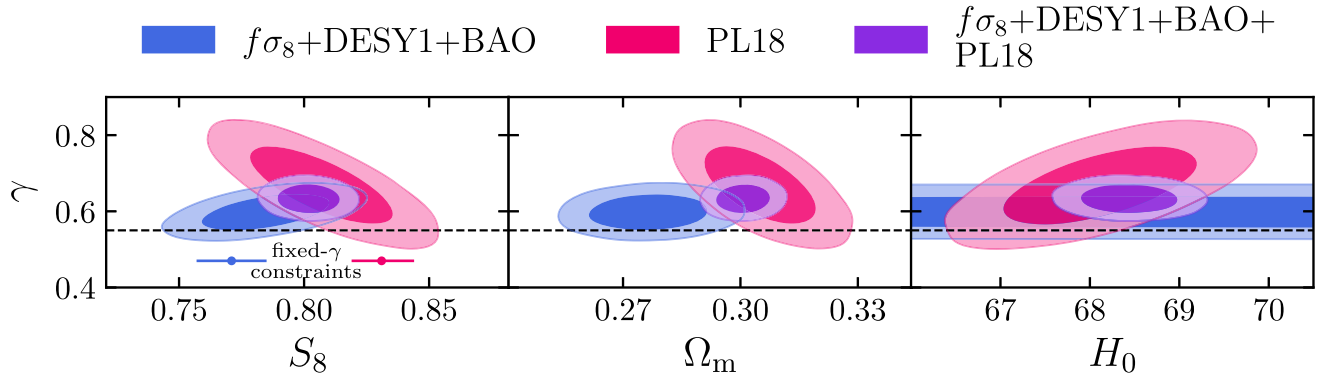


FIG. 3. 68% and 95% marginalized constraints on parameters in the concordance model allowing for a free growth index γ , from $f\sigma_8 + \text{DESY1} + \text{BAO}$ (blue), PL18 alone (red), and $f\sigma_8 + \text{DESY1} + \text{BAO} + \text{PL18}$ (violet). Contours contain 68% and 95% of the corresponding projected 2D constraints. The horizontal black dashed lines mark the concordance model prediction of $\gamma = 0.55$. The horizontal bars in the $\gamma - S_8$ panel indicate the 68% limits on S_8 for a fixed $\gamma = 0.55$ (see text); they are vertically offset from $\gamma = 0.55$ for visibility.

Ω_m or H_0 , by different data combinations. Notably, the $S_8 - \gamma$ panel indicates a potential solution to the S_8 tension: A higher growth index ($\gamma \simeq 0.65$) implies a higher S_8 value in the probes of large-scale structure. Specifically, the $f\sigma_8 + \text{DESY1} + \text{BAO}$ combination yields $S_8 = 0.784^{+0.017}_{-0.016}$, while in the standard ΛCDM (with $\gamma \equiv 0.55$) $S_8 = 0.771^{+0.014}_{-0.014}$. Conversely, Planck now prefers a lower amplitude of fluctuations ($S_8 = 0.807^{+0.019}_{-0.019}$) than it does in ΛCDM ($S_8 = 0.831^{+0.013}_{-0.012}$). Consequently, the “ S_8 tension” between the measurements of S_8 in the galaxy clustering and gravitational lensing versus that in Planck decreases from 3.2σ to 0.9σ , as measured by the S_8 difference divided by errors added in quadrature.

Allowing curvature to vary.—Relaxing the assumption of spatial flatness changes the expansion history and the concordance prediction for the growth history [69,70]. An immediate question is whether the apparent preference for a higher growth index and a slower growth rate is the same effect as the apparent preference for a nonzero curvature found by the Planck 2018 analysis that, by using temperature and polarization data, found $\Omega_K = -0.044^{+0.018}_{-0.015}$ ([3]; see also Refs. [71–73]).

Allowing both the curvature and growth index to vary, we observe a trade-off between Ω_K and γ , as shown in Fig. 4 using only Planck CMB temperature and polarization data (henceforth, PL18 temp + pol). The data clearly prefer either a positively curved space, i.e., $\Omega_K < 0$, or growth suppressed relative to the GR prediction, i.e., $\gamma > 0.55$; the flat model with $\gamma = 0.55$ has a worse fit than the best-fit model by $\Delta\chi^2 = -6.9$.

We next focus on two limits of the results shown in Fig. 4: (a) varying Ω_K while fixing $\gamma = 0.55$ (which reproduces the standard analysis from the Planck paper, also finding $\Omega_K = -0.044$) and (b) fixing $\Omega_K = 0$ while varying γ . We are particularly interested in comparing the fit of these two models. We find that the model with free

curvature fits the PL18 temp + pol data marginally better than the model with free γ ($\Delta\chi^2 = -1.3$). Including PL18 CMB lensing reconstruction likelihood leads to $\Delta\chi^2 = 0.7$ in favor of the free- γ model. Overall, we conclude that both models fit the PL18 data equally well.

Recall that the feature in the PL18 temp + pol data driving the preference for $\Omega_K < 0$ is essentially the same one that favors a high CMB lensing amplitude, i.e., $A_{\text{lens}} > 1$ [3,56,74]. Does the cosmological model with a high γ produce similar features in the CMB power spectra to those with $\Omega_K < 0$ or $A_{\text{lens}} > 1$? The answer is affirmative, as shown in Fig. 5 where we compare the residuals in the CMB TT power spectrum of (a) the PL18 data, (b) the best-fit flat model with γ , (c) the best-fit model with curvature but fixed $\gamma = 0.55$, and (d) the best-fit flat model with A_{lens} but fixed $\gamma = 0.55$, all relative to that of the best-fit concordance model. All three best-fit model

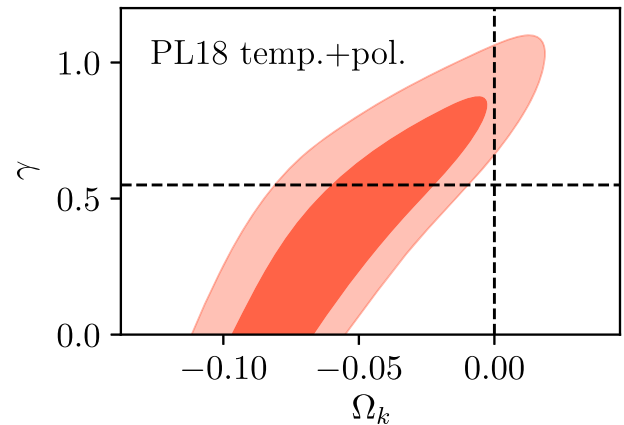


FIG. 4. Degeneracy between γ and Ω_K in the PL18 temp + pol analysis when both parameters are allowed to vary. Contours show the 68% and 95% credible intervals. The dashed lines mark the point $[\Omega_K = 0, \gamma = 0.55]$ corresponding to the concordance flat ΛCDM model.

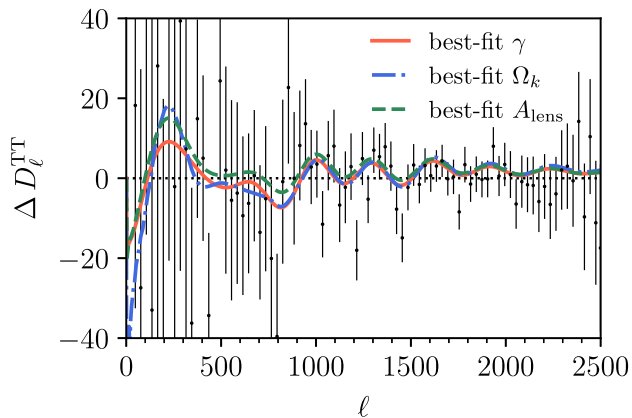


FIG. 5. Residuals in the CMB TT power spectrum $D_\ell \equiv \ell(\ell+1)C_\ell/(2\pi)$ between the best-fit model with free γ (orange), best-fit model with curvature (blue), and best-fit model with free CMB lensing amplitude A_{lens} (green). The data points and error bars represent the Planck 2018 (binned) TT power spectrum residuals and the 68% uncertainties. All residuals are computed with respect to the best-fit concordance model.

residuals display the same oscillatory pattern that closely follows the oscillations in the data residuals. The similarity between the best-fit models with $\gamma > 0.55$ [case (b)] and with $A_{\text{lens}} > 1$ [case (d)] in the CMB power spectra is not entirely surprising: A higher γ encodes a lower growth rate $f(a)$ and, for a fixed amount of structure observed today, a higher growth (relative to standard growth $\gamma = 0.55$) in the recent past [see Eq. (3)]. This in turn implies a higher lensing amplitude; thus, it has a qualitatively similar effect as $A_{\text{lens}} > 1$. We illustrate the effect of γ on the lensing potential power spectrum in the Supplemental Material [63] (see also Ref. [75]).

Summary and discussion.—In this Letter, we have presented new constraints on the growth rate using a combination of Planck, DES, BAO, redshift-space distortion, and peculiar velocity measurements. The constraints from different data combinations are consistent with one another within 1σ . Our constraints exclude the predictions of the flat Λ CDM model in GR at the statistical significance of 3.7σ , indicating a suppression of growth rate during the dark-energy-dominated epoch.

Further, we have demonstrated that cosmological models with a high γ resolve two known tensions in cosmology. First, allowing for a suppressed growth removes the need for negative curvature indicated by the PL18 temp + pol data; in fact, the best-fit flat model with free γ fits the data equally well as the best-fit model with standard growth and negative curvature, producing highly similar features in the TT power spectrum. Second, the discrepancy in the measured amplitude of mass fluctuations parameter S_8 from the PL18 data and that from the large-scale structure data can be reconciled with a high- γ model. Our findings indicate that these cosmological tensions can be interpreted as evidence of growth suppression.

A late-time linear growth suppression is not straightforward to achieve in modified theories of gravity, particularly if the expansion history is similar to that in the concordance model [76–78] as our constraints indicate. Nevertheless, there is sufficient freedom in the space of modified-gravity theory (within a subclass of Horndeski models, e.g., Refs. [79–82]) to do so [83]. Probing such modified-gravity theories should be within the reach of future surveys and experiments [82,86,87]. Specifically, upcoming large-scale structure data [88–93] will improve $f\sigma_8$ data both in terms of measurement precision and redshift coverage. In parallel, forthcoming CMB measurements [65,94–96] with higher resolution and sensitivity will play a significant role in pinning down the expansion history and growth rate. In this era of high-precision large-scale structure and CMB measurements, joint analyses of these datasets will hold the key to confirming any evidence for physics beyond the standard model.

We are grateful to Eiichiro Komatsu, Eric Linder, Jessie Muir, Fabian Schmidt, and the three anonymous referees for their valuable comments on the manuscript. M.N. thanks Alex Mead for helpful conversations on details and modifications of HMCODE-2020. We thank Alex Barreira, Elisa Ferreira, Shaun Hotchkiss, Jiamin Hou, Cullan Howlett, Mike Hudson, Stéphanie Ilić, Johannes Lange, and Antony Lewis for useful discussions. We acknowledge Cosmology Talks and their mini-workshop that bring community experts together to discuss results in this work and their implications. We acknowledge support from the Leinweber Center for Theoretical Physics, NASA grant under Contract No. 19-ATP19-0058, DOE under Contract No. DE-FG02-95ER40899, and the University of Michigan Research Computing Package. Our analysis was performed on the Greatlakes HPC cluster maintained by the Advanced Research Computing division, U of M Information and Technology Service. M.N. thanks John Thiels and Mark Champe for going above and beyond during their service. This work was initiated at the Aspen Center for Physics, which was supported by the National Science Foundation Grant No. PHY-1607611. We thank the Aspen Center for their hospitality.

*nguyenmn@umich.edu

†huterer@umich.edu

*ywwen@umich.edu

- [1] E. Abdalla *et al.*, *J. High Energy Astrophys.* **34**, 49 (2022).
- [2] A. G. Riess, W. Yuan, L. M. Macri, D. Scolnic, D. Brout, S. Casertano, D. O. Jones, Y. Murakami, G. S. Anand, L. Breuval, T. G. Brink, A. V. Filippenko, S. Hoffmann, S. W. Jha, W. D’arcy Kenworthy, J. Mackenty, B. E. Stahl, and W. Zheng, *Astrophys. J. Lett.* **934**, L7 (2022).
- [3] N. Aghanim *et al.* (Planck Collaboration), *Astron. Astrophys.* **641**, A6 (2020); **652**, C4(E) (2021).
- [4] E. Di Valentino *et al.*, *Astropart. Phys.* **131**, 102604 (2021).

- [5] D. Huterer, *Astron. Astrophys. Rev.* **31**, 2 (2023).
- [6] E. J. Ruiz and D. Huterer, *Phys. Rev. D* **91**, 063009 (2015).
- [7] J. L. Bernal, L. Verde, and A. J. Cuesta, *J. Cosmol. Astropart. Phys.* **02** (2016) 059.
- [8] A. Johnson, C. Blake, J. Dossett, J. Koda, D. Parkinson, and S. Joudaki, *Mon. Not. R. Astron. Soc.* **458**, 2725 (2016).
- [9] M. Moresco and F. Marulli, *Mon. Not. R. Astron. Soc.* **471**, L82 (2017).
- [10] S. Basilakos and F. K. Anagnostopoulos, *Eur. Phys. J. C* **80**, 212 (2020).
- [11] K. Said, M. Colless, C. Magoulas, J. R. Lucey, and M. J. Hudson, *Mon. Not. R. Astron. Soc.* **497**, 1275 (2020).
- [12] C. García-García, J. Ruiz-Zapatero, D. Alonso, E. Bellini, P. G. Ferreira, E.-M. Mueller, A. Nicola, and P. Ruiz-Lapuente, *J. Cosmol. Astropart. Phys.* **10** (2021) 030.
- [13] J. Ruiz-Zapatero, C. García-García, D. Alonso, P. G. Ferreira, and R. D. P. Grumitt, *Mon. Not. R. Astron. Soc.* **512**, 1967 (2022).
- [14] M. White, R. Zhou, J. DeRose, S. Ferraro, S.-F. Chen, N. Kokron, S. Bailey, D. Brooks, J. García-Bellido, J. Guy, K. Honscheid, R. Kehoe, A. Kremin, M. Levi, N. Palanque-Delabrouille, C. Poppett, D. Schlegel, and G. Tarle, *J. Cosmol. Astropart. Phys.* **02** (2022) 007.
- [15] S.-F. Chen, M. White, J. DeRose, and N. Kokron, *J. Cosmol. Astropart. Phys.* **07** (2022) 041.
- [16] T. M. C. Abbott *et al.* (DES Collaboration), *Phys. Rev. D* **107**, 083504 (2023).
- [17] S. Wang, L. Hui, M. May, and Z. Haiman, *Phys. Rev. D* **76**, 063503 (2007).
- [18] L. Guzzo *et al.*, *Nature (London)* **451**, 541 (2008).
- [19] J. Dossett, M. Ishak, J. Moldenhauer, Y. Gong, A. Wang, and Y. Gong, *J. Cosmol. Astropart. Phys.* **04** (2010) 022.
- [20] M. J. Hudson and S. J. Turnbull, *Astrophys. J. Lett.* **751**, L30 (2012).
- [21] D. Rapetti, C. Blake, S. W. Allen, A. Mantz, D. Parkinson, and F. Beutler, *Mon. Not. R. Astron. Soc.* **432**, 973 (2013).
- [22] A. Pouri, S. Basilakos, and M. Plionis, *J. Cosmol. Astropart. Phys.* **08** (2014) 042.
- [23] S. Alam, S. Ho, and A. Silvestri, *Mon. Not. R. Astron. Soc.* **456**, 3743 (2016).
- [24] J. Ruiz-Zapatero, B. Stözlner, B. Joachimi, M. Asgari, M. Bilicki, A. Dvornik, B. Giblin, C. Heymans, H. Hildebrandt, A. Kannawadi *et al.*, *Astron. Astrophys.* **655**, A11 (2021).
- [25] J. Muir *et al.* (DES Collaboration), *Phys. Rev. D* **103**, 023528 (2021).
- [26] U. Andrade, D. Anbajagane, R. von Martens, D. Huterer, and J. Alcaniz, *J. Cosmol. Astropart. Phys.* **11** (2021) 014.
- [27] P. J. E. Peebles, *The Large-Scale Structure of the Universe* (Princeton University Press, Princeton, NJ, 1980).
- [28] F. Bernardeau, S. Colombi, E. Gaztañaga, and R. Scoccimarro, *Phys. Rep.* **367**, 1 (2002).
- [29] P. J. E. Peebles, *Astrophys. J.* **205**, 318 (1976).
- [30] A. P. Lightman and P. L. Schechter, *Astrophys. J. Suppl. Ser.* **74**, 831 (1990).
- [31] A. Cooray, D. Huterer, and D. Baumann, *Phys. Rev. D* **69**, 027301 (2004).
- [32] J. N. Fry, *Phys. Lett.* **158B**, 211 (1985).
- [33] L.-M. Wang and P. J. Steinhardt, *Astrophys. J.* **508**, 483 (1998).
- [34] E. V. Linder, *Phys. Rev. D* **72**, 043529 (2005).
- [35] E. V. Linder and R. N. Cahn, *Astropart. Phys.* **28**, 481 (2007).
- [36] Y. Gong, *Phys. Rev. D* **78**, 123010 (2008).
- [37] A. Lewis, A. Challinor, and A. Lasenby, *Astrophys. J.* **538**, 473 (2000).
- [38] C. Howlett, A. Lewis, A. Hall, and A. Challinor, *J. Cosmol. Astropart. Phys.* **04** (2012) 027.
- [39] T. M. C. Abbott *et al.* (Dark Energy Survey Collaboration), *Phys. Rev. D* **98**, 043526 (2018).
- [40] Code available at this fork of CAMB: https://github.com/MinhMPA/CAMB_GammaPrime_Growth.
- [41] The integrated Sachs-Wolfe effect [42,43], a secondary CMB anisotropy sourced by gravitational redshift, is also affected by γ and Eq. (4). We do not consider that signal here.
- [42] R. K. Sachs and A. M. Wolfe, *Astrophys. J.* **147**, 73 (1967).
- [43] J. Carron, A. Lewis, and G. Fabbian, *Phys. Rev. D* **106**, 103507 (2022).
- [44] F. Beutler, C. Blake, M. Colless, D. H. Jones, L. Staveley-Smith, G. B. Poole, L. Campbell, Q. Parker, W. Saunders, and F. Watson, *Mon. Not. R. Astron. Soc.* **423**, 3430 (2012).
- [45] D. Huterer, D. Shafer, D. Scolnic, and F. Schmidt, *J. Cosmol. Astropart. Phys.* **05** (2017) 015.
- [46] S. S. Boruah, M. J. Hudson, and G. Lavaux, *Mon. Not. R. Astron. Soc.* **498**, 2703 (2020).
- [47] R. J. Turner, C. Blake, and R. Ruggeri, *Mon. Not. R. Astron. Soc.* **518**, 2436 (2023).
- [48] C. Blake *et al.*, *Mon. Not. R. Astron. Soc.* **415**, 2876 (2011).
- [49] C. Blake *et al.* (GAMA Collaboration), *Mon. Not. R. Astron. Soc.* **436**, 3089 (2013).
- [50] C. Howlett, A. J. Ross, L. Samushia, W. J. Percival, and M. Manera, *Mon. Not. R. Astron. Soc.* **449**, 848 (2015).
- [51] T. Okumura *et al.*, *Publ. Astron. Soc. Jpn.* **68**, 38 (2016).
- [52] A. Pezzotta *et al.*, *Astron. Astrophys.* **604**, A33 (2017).
- [53] S. Alam *et al.* (eBOSS Collaboration), *Phys. Rev. D* **103**, 083533 (2021).
- [54] Likelihood and data available at <https://github.com/MinhMPA/cobaya>.
- [55] N. Aghanim *et al.* (Planck Collaboration), *Astron. Astrophys.* **641**, A8 (2020).
- [56] N. Aghanim *et al.* (Planck Collaboration), *Astron. Astrophys.* **641**, A5 (2020).
- [57] F. Beutler, C. Blake, M. Colless, D. H. Jones, L. Staveley-Smith, L. Campbell, Q. Parker, W. Saunders, and F. Watson, *Mon. Not. R. Astron. Soc.* **416**, 3017 (2011).
- [58] A. J. Ross, L. Samushia, C. Howlett, W. J. Percival, A. Burden, and M. Manera (BOSS Collaboration), *Mon. Not. R. Astron. Soc.* **449**, 835 (2015).
- [59] S. Alam *et al.* (BOSS Collaboration), *Mon. Not. R. Astron. Soc.* **470**, 2617 (2017).
- [60] https://cobaya.readthedocs.io/en/latest/likelihood_bao.html.
- [61] J. Torrado and A. Lewis, *J. Cosmol. Astropart. Phys.* **05** (2021) 057.
- [62] A. Lewis, arXiv:1910.13970.
- [63] See Supplemental Material at <http://link.aps.org/supplemental/10.1103/PhysRevLett.131.111001> for model goodness of fits, implementation details, and robustness tests.
- [64] H. Jeffreys, *Theory of Probability* (Oxford University Press, New York, 1939).

- [65] S. Aiola *et al.* (ACT Collaboration), *J. Cosmol. Astropart. Phys.* **12** (2020) 047.
- [66] C. Heymans *et al.* (Kilo-Degree Survey Collaboration), *Astron. Astrophys.* **646**, A140 (2021).
- [67] A. Amon *et al.*, *Mon. Not. R. Astron. Soc.* **518**, 477 (2023).
- [68] A. Leauthaud *et al.*, *Mon. Not. R. Astron. Soc.* **510**, 6150 (2022).
- [69] M. J. Mortonson, W. Hu, and D. Huterer, *Phys. Rev. D* **79**, 023004 (2009).
- [70] Y. Gong, M. Ishak, and A. Wang, *Phys. Rev. D* **80**, 023002 (2009).
- [71] E. Di Valentino, A. Melchiorri, and J. Silk, *Nat. Astron.* **4**, 196 (2020).
- [72] W. Handley, *Phys. Rev. D* **103**, L041301 (2021).
- [73] E. Di Valentino, W. Giarè, A. Melchiorri, and J. Silk, *Phys. Rev. D* **106**, 103506 (2022).
- [74] P. A. R. Ade *et al.* (Planck Collaboration), *Astron. Astrophys.* **594**, A13 (2016).
- [75] The preference for the anomalous growth index in PL18 temp.+pol. data ($\Delta\chi^2 = -8.5$ in favor of the free- γ model over the concordance one) decreases once the CMB lensing reconstruction likelihood is included ($\Delta\chi^2 = -2.8$). A similar effect is observed for the case of varying A_{lens} .
- [76] A. Barreira, B. Li, C. M. Baugh, and S. Pascoli, *Phys. Rev. D* **86**, 124016 (2012).
- [77] A. Joyce, L. Lombriser, and F. Schmidt, *Annu. Rev. Nucl. Part. Sci.* **66**, 95 (2016).
- [78] J. A. Kable, G. Benevento, N. Frusciante, A. De Felice, and S. Tsujikawa, *J. Cosmol. Astropart. Phys.* **09** (2022) 002.
- [79] F. Piazza, H. Steigerwald, and C. Marinoni, *J. Cosmol. Astropart. Phys.* **05** (2014) 043.
- [80] L. Pèrenon, F. Piazza, C. Marinoni, and L. Hui, *J. Cosmol. Astropart. Phys.* **11** (2015) 029.
- [81] L. Perenon, J. Bel, R. Maartens, and A. de la Cruz-Dombriz, *J. Cosmol. Astropart. Phys.* **06** (2019) 020.
- [82] Y. Wen, N.-M. Nguyen, and D. Huterer, arXiv:2304.07281.
- [83] A scale-dependent suppression would open up more possibilities, e.g., alternative models of dark matter [84,85].
- [84] G. F. Abellán, R. Murgia, V. Poulin, and J. Laval, *Phys. Rev. D* **105**, 063525 (2022).
- [85] K. K. Rogers, R. Hložek, A. Laguë, M. M. Ivanov, O. H. E. Philcox, G. Cabass, K. Akitsu, and D. J. E. Marsh, *J. Cosmol. Astropart. Phys.* **06** (2023) 023.
- [86] N. Frusciante, S. Peirone, S. Casas, and N. A. Lima, *Phys. Rev. D* **99**, 063538 (2019).
- [87] L. Perenon, S. Ilić, R. Maartens, and A. de la Cruz-Dombriz, *Astron. Astrophys.* **642**, A116 (2020).
- [88] E. da Cunha *et al.* (Taipan Collaboration), *Pub. Astron. Soc. Aust.* **34**, e047 (2017).
- [89] K. Gebhardt *et al.* (HETDEX Collaboration), *Astrophys. J.* **923**, 217 (2021).
- [90] D. J. Schlegel *et al.* (DESI Collaboration), arXiv:2209.03585.
- [91] M. Takada *et al.* (PFS Collaboration), *Publ. Astron. Soc. Jpn.* **66**, R1 (2014).
- [92] R. Laureijs *et al.* (Euclid Collaboration), arXiv:1110.3193.
- [93] D. J. Schlegel *et al.*, arXiv:2209.04322.
- [94] P. Ade *et al.* (Simons Observatory Collaboration), *J. Cosmol. Astropart. Phys.* **02** (2019) 056.
- [95] K. N. Abazajian *et al.* (CMB-S4 Collaboration), arXiv:1610.02743.
- [96] E. Allys *et al.* (LiteBIRD Collaboration), *Prog. Theor. Exp. Phys.* **2023**, 042F01 (2023).